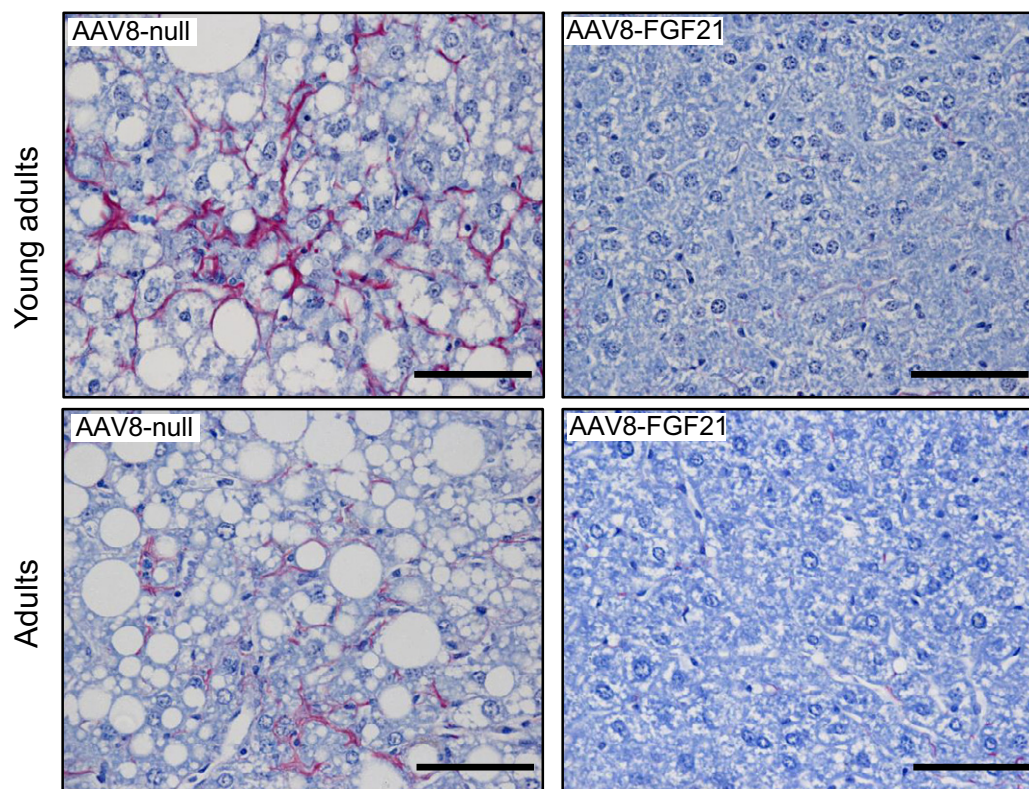


## Expanded View Figures



**Figure EV1. AAV8-hAAT-FGF21 treatment improves liver fibrosis.**

Analysis of hepatic fibrosis through PicroSirius staining in animals fed a HFD that received  $5 \times 10^{10}$  vg/mouse of either AAV8-hAAT-null or AAV8-hAAT-FGF21 vectors. AAV8-hAAT-FGF21 treatment (*right panels*) markedly decreased the detection of collagen fibers that were readily detectable (in red) in animals treated with the null vector (*left panels*). Scale bars: 50  $\mu$ m.

**Figure EV2. AAV8-hAAT-FGF21-mediated reversal of islet hyperplasia.**

- A Fasted glucagon levels in the group of animals that initiated the HFD feeding and received FGF21 vectors as young adults.  
 B Representative images of the immunostaining against insulin in pancreas sections from animals that received  $5 \times 10^{10}$  vg/mouse of AAV8-hAAT-FGF21 as adults. Scale bars: 400  $\mu$ m. Inset scale bars: 100  $\mu$ m.  
 C Representative images of the double immunostaining against insulin (in green) and glucagon (in red) in pancreas sections from animals that received  $5 \times 10^{10}$  vg/mouse of AAV8-hAAT-FGF21 as young adults (*upper panel*) or adults (*lower panel*). Scale bars: 100  $\mu$ m.

Data information: All values are expressed as mean  $\pm$  SEM. In (A), young adults: AAV8-hAAT-null chow ( $n = 10$  animals), AAV8-hAAT-null HFD ( $n = 10$ ), AAV8-hAAT-FGF21 HFD  $1 \times 10^{10}$  vg ( $n = 9$ ), and  $5 \times 10^{10}$  vg ( $n = 10$ ). In (A), data were analyzed by one-way ANOVA with Tukey's post hoc correction.  $^{\#}P < 0.05$  and  $^{\#\#}P < 0.01$  versus the HFD-fed null-injected group. HFD, High-fat diet.

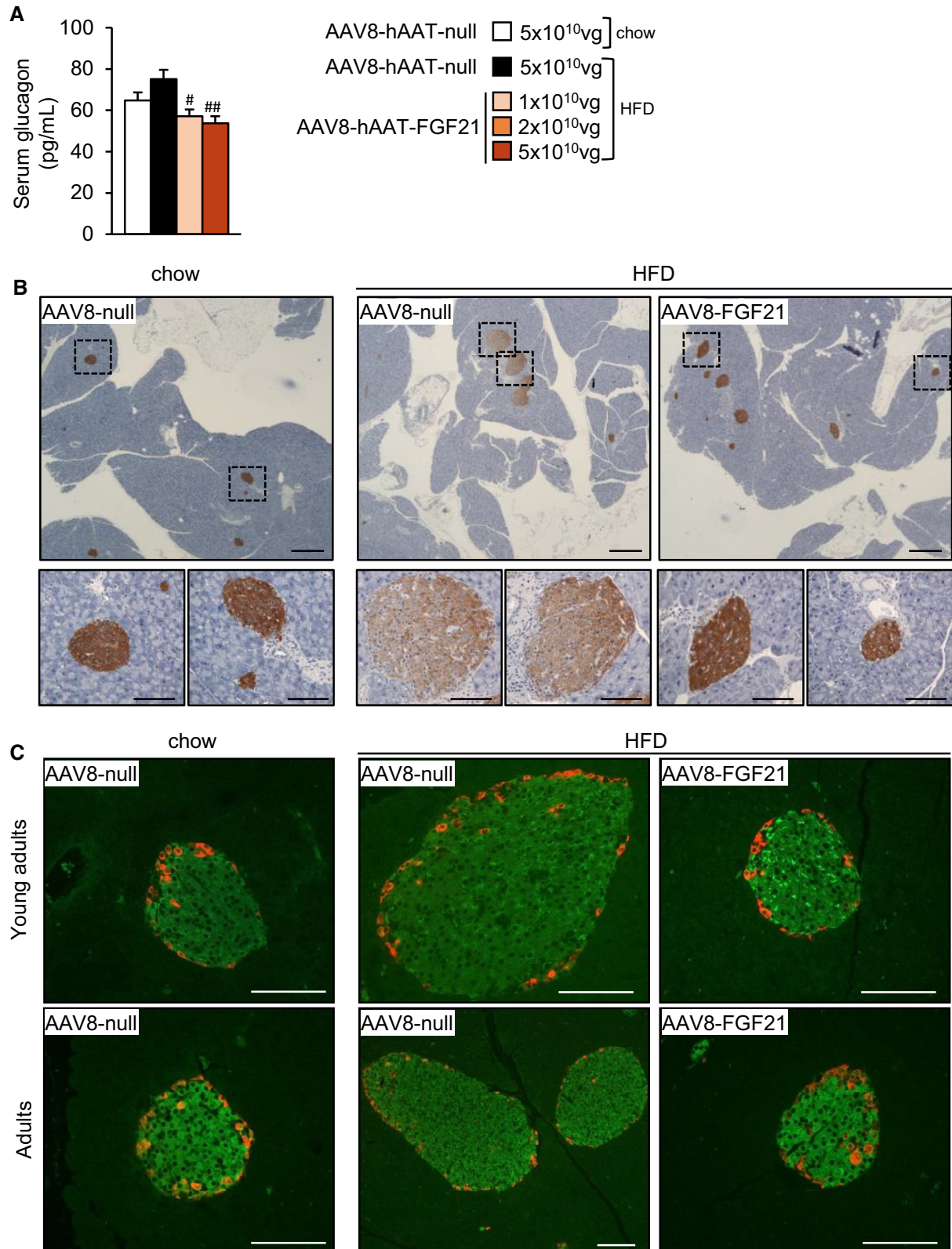


Figure EV2.

**Figure EV3. No bone abnormalities were observed in AAV8-hAAT-FGF21-treated animals.**

The long-term effects of FGF21 gene transfer on bones were studied by comparison of HFD-fed mice treated with the highest dose ( $5 \times 10^{10}$  vg/mouse) of FGF21 vectors as young adults or adults with null-injected, chow or HFD-fed animals.

A Total naso-anal length.

B Tibial length.

C–O Micro-computed tomography ( $\mu$ CT) analysis of the epiphysis (C–J) and the diaphysis (K–O) of tibiae obtained at the time of sacrifice, that is, when animals were 18 months of age, from HFD-fed mice administered with either null or FGF21-encoding AAV vectors.

P, Q Circulating IGFBP1 (P) and IGF1 (Q) levels measured by ELISA.

Data information: All data represent the mean  $\pm$  SEM. In (A, P, Q), Young adults: AAV8-hAAT-null chow ( $n = 10$  animals), AAV8-hAAT-null HFD ( $n = 8$ ), AAV8-hAAT-FGF21 HFD  $1 \times 10^{10}$  vg ( $n = 9$ ), and  $5 \times 10^{10}$  vg ( $n = 8$ ). Adults: AAV8-hAAT-null chow ( $n = 7$ ), AAV8-hAAT-null HFD ( $n = 7$ ), AAV8-hAAT-FGF21 HFD  $1 \times 10^{10}$  vg ( $n = 7$ ),  $2 \times 10^{10}$  vg ( $n = 8$ ), and  $5 \times 10^{10}$  vg ( $n = 7$ ). In (B–O),  $n = 4$  animals/group. In (A, B, P, Q), data were analyzed by one-way ANOVA with Tukey's post hoc correction. In (C–O), data were analyzed by unpaired Student's *t*-test. **\*\*** $P < 0.01$  and **\*\*\*** $P < 0.001$  versus the chow-fed null-injected group. HFD, high-fat diet; BMD, bone mineral density; BMC, bone mineral content; BV, bone volume; BV/TV, bone volume/tissue volume ratio; BS/BV, bone surface/bone volume ratio; Tb.N, trabecular number; Tb.Th, trabecular thickness; Tb.Sp, trabecular separation.

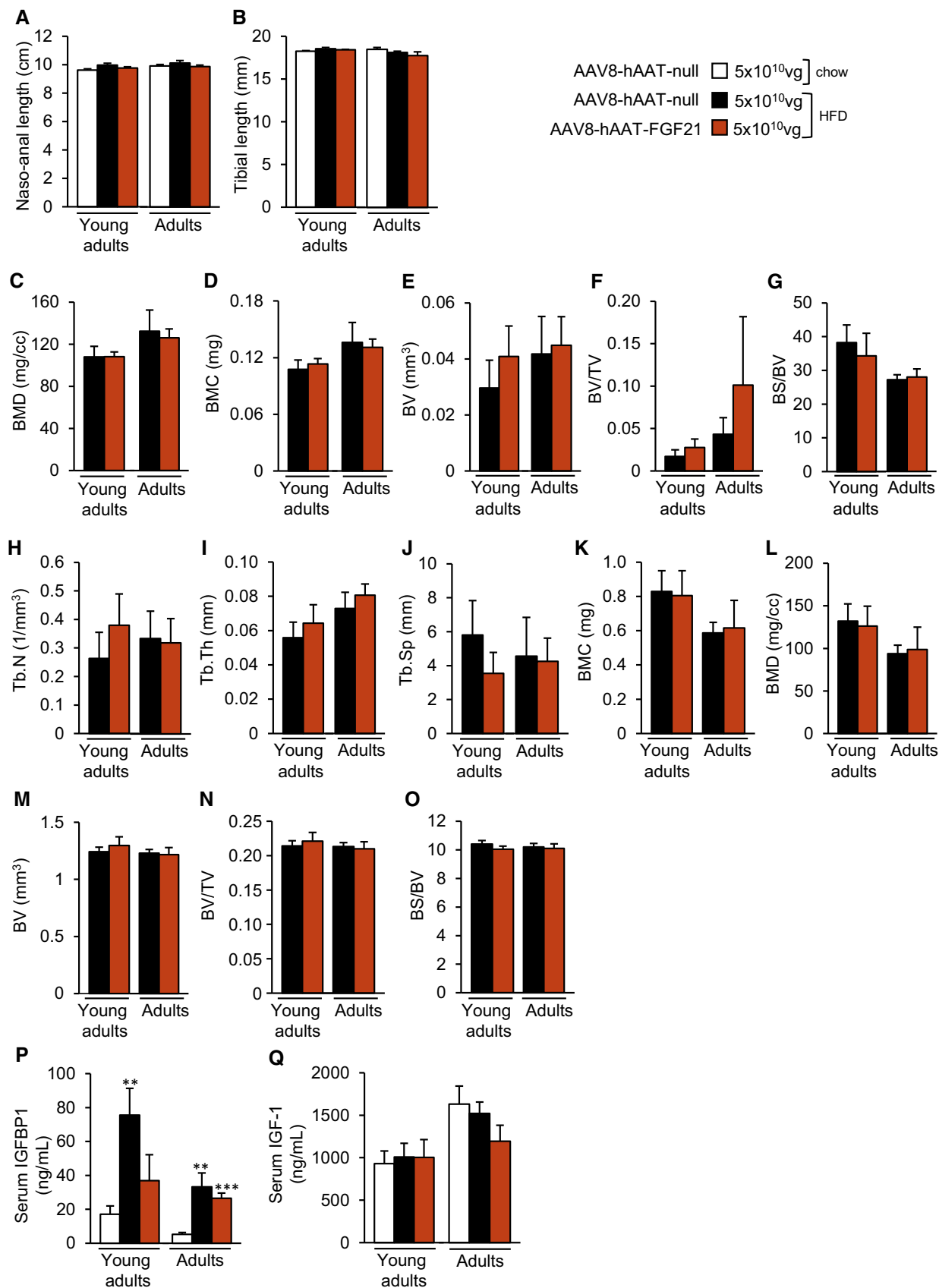


Figure EV3.